frontiers | Frontiers in Environmental Engineering

TYPE Original Research
PUBLISHED 24 March 2023
DOI 10.3389/fenve.2023.1167552

OPEN ACCESS

EDITED BY
Shujuan Zhang,
Nanjing University, China

REVIEWED BY
Seyma Ozkara-Aydinoglu,
Beykent University, Türkiye
Vesna Krstic,
Mining and Metallurgy Institute Bor, Serbia

*CORRESPONDENCE
Kui Qiu,
zhih98liu@163.com

SPECIALTY SECTION
This article was submitted to Environmental Catalysis, a section of the journal Frontiers in Environmental Engineering

RECEIVED 16 February 2023
ACCEPTED 13 March 2023
PUBLISHED 24 March 2023

CITATION
Liu Z, Chen Z, Chen Q, Liu L, Wang Y, Shu P, Zhong Y, Sun Z and Qiu K (2023), Heterogeneous catalytic oxidation regeneration of desulfurization-rich liquor with Fe^{3+} modified chitosan. *Front. Environ. Eng.* 2:1167552. doi: 10.3389/fenve.2023.1167552

Heterogeneous catalytic oxidation regeneration of desulfurization-rich liquor with Fe^{3+} modified chitosan

Zhihao Liu[1], Zhijie Chen[2], Qian Chen[2], Luwei Liu[1], Yingjie Wang[1], Peng Shu[1], Yu Zhong[1], Zeqin Sun[1] and Kui Qiu[1]*

[1]School of Chemistry and Chemical Engineering, Chongqing University of Science and Technology, Chongqing, China, [2]Centre for Technology in Water and Wastewater, School of Civil and Environmental Engineering, University of Technology Sydney, Ultimo, NSW, Australia

To solve the problem of pipeline blockage caused by sulfur deposition in industrial gas wet oxidative desulfurization operations, this study developed an iron-modified chitosan catalyst for the catalytic oxidation regeneration of conventional wet oxidative desulfurization-rich liquids. Detailed characterization results show that Fe^{3+} species are successfully coordinated with the chitosan substrate. The results of desulfurization and regeneration experiments showed that the Fe^{3+}-modified chitosan could effectively regenerate the desulfurization waste stream and remain stable in the acidic desulfurization stream. The powdered iron-based modified chitosan catalyst prepared with a mass ratio of chitosan to $FeCl_3$ of 1:5 and glutaraldehyde of 12.5% by mass has better catalytic performance than the microbead counterpart. The regeneration performance of the catalyst was evaluated by the desulfurization performance of the regenerated desulfurization solution. The iron-based modified chitosan shows a good regeneration performance, and the loss of Fe content is less than 1.5% after five runs. This study provides an efficient way to develop cost-effective catalysts for the regeneration of wet oxidative desulfurization-rich liquids.

KEYWORDS

catalytic oxidation, desulfurization, chitosan, regeneration, Fe^{3+}

1 Introduction

As a toxic and harmful gas, hydrogen sulfide (H_2S) in industrial gas (natural gas, biogas, etc.) poses serious environmental and human hazards in addition to severe corrosion of metal pipelines and production equipment (Liu et al., 2023a). Various desulfurization processes have been developed according to the complex desulfurization scenarios. For small- and medium-scale gas desulfurization, solid adsorption and wet oxidation desulfurization are the widely used. The former is generally applicable to low-sulfur gas purification and the latter one suffers from low sulfur capacity, easy solvent degradation, affluent generation, and poor sulfur quality (Qiu et al., 2022). In addition, the most widely used organic iron-based wet desulfurization solution can easily lead to H_2S oxidation and thereby lead to sulfur blockage in the reactor and pipeline accumulation (Liu et al., 2022). Currently, this phenomenon is widespread in high-pressure and high-sulfur-content scenarios. Therefore, for small to medium-scale industrial gas desulfurization, there are a

few cases where wet oxidation desulfurization is directly utilized at high H_2S concentrations and high pressures (Vogt and Weckhuysen, 2022). The use of multiple process combinations for desulfurization and sulfur recovery complicatesthe process for the many scattered sulfur-bearing single wells around the world.

To address this problem, we propose a stepwise desulfurization-regeneration scheme. More specifically, it is assumed that the desulfurization solution absorbs the H_2S in a non-redox form, and after the rich solution enters the regeneration tower, modified solid catalyst particles containing Fe^{3+} are added, and the air is introduced to oxidize the HS^- in the rich solution of desulfurization to S monomers. This form of non-homogeneous catalytic oxidation can avoid the generation of sulfur particles in the absorption stage and solve the sulfur plugging problem in the wet oxidation desulfurization operation. Its application to small-scale high-pressure industrial gas desulfurization can greatly simplify the well site desulfurization process and effectively achieve green, efficient, and economic sulfur-bearing wellhead gas capacity release (Gu et al., 2008). The antimony-based organic non-aqueous phase desulfurization system developed in our previous work (Liu et al., 2022) is effective in removing H_2S from gas streams through ligand absorption.

Chitosan (CS), known as chitosan-amine or deacetylated chitosan, is a product of the deacetylation of chitinand is the only basic polysaccharide among natural polysaccharides (Dash et al., 2011). Chitosan has a large number of reactive groups such as -OH and -NH_2 in its molecule. The flat-voltage bond structure in the chitosan molecule enables it to interact with a variety of metal ions in coordination, which can provide nucleation sites for the formation of catalysts, with high adsorption efficiency and excellent chelating properties. Microspheres with a high specific surface area are more suitable for efficient adsorbents compared to conventional fibers, membranes, and resins (He et al., 2016). Therefore, chitosan is considered a functional biomaterial with potential applications. In addition, chitosan has the general properties of polymeric compounds in solution, being insoluble in water, alkalis, and organic solvents in general, and chemically stable (Lei et al., 2022).

In view of this, we developed a Fe^{3+}-modified chitosan catalyst for the non-homogeneous catalytic oxidation regeneration of desulfurization solution. XRD and FTIR techniques were used to characterize the structure of the catalyst samples, and the microscopic morphology of the samples was observed by SEM. The regeneration performance of the catalyst for the desulfurization of the desulfurization solution and the change of ORP (oxidation-reduction potential) value of the solution after regeneration were investigated. This work aims to provide a new solution for more desulfurization scenarios (natural gas, biogas, etc.).

2 Experimental

2.1 Materials and reagents

Anhydrous ethanol, ferric chloride, glacial acetic acid, 50% glutaraldehyde, sodium hydroxide (analytically pure), all purchased from Chengdu Jinshan Chemical Reagent Co. Chitosan (CS, deacetylation degree ≥95%) was obtained from Jiangsu Golden Shell Pharmaceutical). Antimony-based desulfurization agent was self-prepared.

H_2S standard gas, 5% H_2S/95% N_2 (Chongqing Lituo Gas Co.), O_2 standard gas, 99.9% O_2 (Chongqing Yongfa Gas Co.).

2.2 Apparatus and instruments

The variations of the functional groups on the fiber surface were observed using a Fourier transform infrared spectrometer (FT-IR, KBr, 4000–500 cm1, BRUKE TENS OR27, Germany). The solution OPR value was determined using a PHS-3E pH meter from Shanghai Yidian Scientific Instrument Co. (China) The crystal structure of the sample was analyzed using a SmartLab-9 type X-ray diffraction (XRD) analyzer (RIKEN, Japan). The surface morphology of the samples was observed using an FSEM-type scanning electron microscope analyzer (FEI, USA), and the elemental content of the sample surface was determined. Determination of Fe element in catalysts by inductively coupled plasma emission spectrometer/mass spectrometer (ICP-OES).

2.3 Preparation of Fe^{3+} modified chitosan

Firstly, all samples were soaked in NMP (N-Methyl-pyrrolidone) solvent for 24 h before the experiments, and it was proved that all samples were insoluble in the desulfurization solution. Taking an appropriate amount of chitosan (CS) and add it to 2% acetic acid solution, stirring until the chitosan was completely dissolved. Then, adding a certain mass of $FeCl_3$ was to the above mixture, stirring well and then left the load for 2 h; then, loading the resting mixed solution into a syringe and slowly dropped it into 2 mol/L sodium hydroxide solution to form iron-based modified chitosan gel microspheres. After that, washing the chitosan gel microspheres with distilled water several times to neutralize them. Then, all of them were placed into a certain concentration of glutaraldehyde solution for cross-linking reaction, and the microspheres were stirred continuously to make full contact with glutaraldehyde for 24 h at room temperature; finally, the cross-linked chitosan microspheres were washed several times with distilled water to neutral, and then dried at 60°C for 24 h. The iron-based modified chitosan microspheres (Fe-CS) were successfully produced.

2.4 Preparation of modified chitosan catalyst

Due to the high density of iron-based modified chitosan microspheres, when the oxygen inflow is slight, many catalyst microspheres will accumulate at the bottom of the U-shaped bubble tube, and only a tiny portion of catalyst microspheres can be suspended in the desulfurization solution. The catalyst cannot fully contact the desulfurization solution, and the regeneration effect is unsatisfactory. For this reason, we prepared iron-based modified chitosan as a powder catalyst. The mixed solution of iron-based chitosan was dropped into 0.5 mol/L sodium hydroxide solution with a syringe, during which the chitosan

FIGURE 1
Fe-CS microspheres (left) and Fe-CS powder (right).

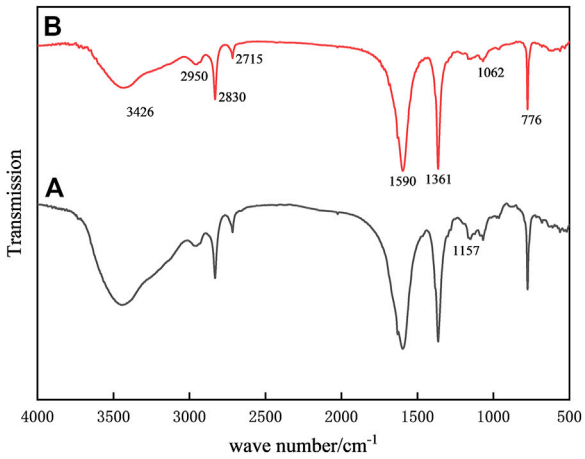

FIGURE 2
FTIR spectra of **(A)** CS and **(B)** Fe-CS.

would gradually disperse in the solution without coalescing into spheres, washed to neutrality and then cross-linked with glutaraldehyde for 24 h. Finally, the dried catalyst was ground into finer iron-based modified chitosan powder through a mortar. As shown in Figure 1, the catalyst after loading Fe^{3+} was obviously reddish compared with the counterpart before the reaction. The powdered catalyst can be better suspended in the desulfurization solution and increase the chance of interaction with S^{2-} (Wang et al., 2022).

2.5 Desulfurization and regeneration experiments

The desulfurization solution used for the experiments was prepared in the laboratory, referring to our previous work (Liu et al., 2022). Its main components were 40 ml of N-methyl pyrrolidone (NMP) and 1 g of antimony chloride ($SbCl_3$). The configured desulfurization solution was stirred well and poured into the bubble reactor, preheated in a water bath at 40°C for 2 min, and the H_2S standard gas was introduced at a volume flow rate of 20 ml/min for the desulfurization experiment, and the experiment was stopped when the mass concentration of tail gas H_2S reached 20 mg/m^3.

2 g of the prepared catalyst was placed in a U-shaped bubble reactor, 40 ml of H_2S-absorbed desulfurization solution was added and regenerated with pure oxygen bubble, the flow rate was set at 200 ml/min, and the ORP of the liquid was measured every 1 h. Separate the desulfurization liquid from the catalyst, and pour the regenerated desulfurization liquid back into the bubble reactor for the second desulfurization experiment. The purification efficiency was plotted with the desulfurization time as the horizontal coordinate and the mass concentration of H_2S in the tail gas as the vertical coordinate. The effect of catalytic oxidation regeneration of the catalyst on the desulfurization-rich liquid was judged according to the desulfurization time of the regenerated desulfurization liquid. The longer the desulfurization time of the solution after regeneration by

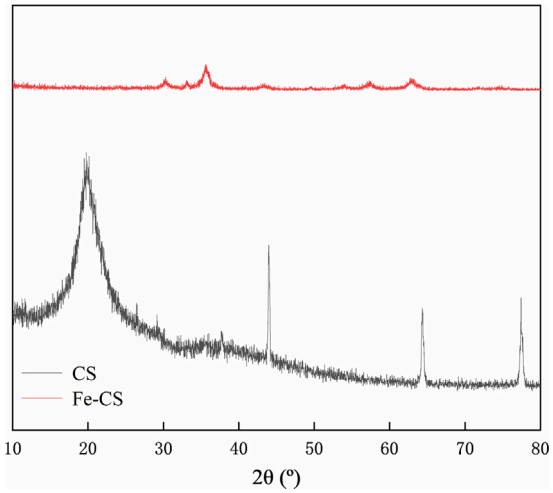

FIGURE 3
XRD analysis of CS and Fe-CS.

catalyst air oxidation, the better the catalytic oxidation regeneration effect of the catalyst on the desulfurization solution.

3 Result and discussion

3.1 Characterization of Fe^{3+} modified chitosan

3.1.1 FTIR analysis

Figure 2 displays the infrared spectra of the samples both before and after alteration. The FTIR spectra of standard chitosan are shown in curve a. Among them, the broad absorption band at 3426 cm^{-1} can be attributed to the stretching vibration of -OH and -NH.while 2950 cm^{-1}, 2830 cm^{-1}, and 2715 cm^{-1} are attributed to the stretching vibration of C-H, 1361 cm^{-1} is the peak of the bending vibration of C-H, respectively (Zheng et al., 2017; Ren et al., 2021); At 1590 cm^{-1}, a clear amide II band appears, which belongs to the bending vibration of N-H, and 1157 cm^{-1} is the peak of the bending vibration of C-H. The amide II band at 1590 cm^{-1} belongs to the bending vibration of N-H, and the peaks at 1157 cm^{-1} and 1062 cm^{-1} belong to the absorption of the C-N stretching vibration (Mohammadi et al., 2019). Compared with the native chitosan, the intensity of the absorption band at 3426 cm^{-1} decreased, indicating that the hydroxyl group of chitosan and the aldehyde group of glutaraldehyde produced acetalization and consumed part of the -OH. In addition, the consumption of the free -NH_2 group by chelation and cross-linking caused the absorption of the C-N stretching vibration at 1157 cm^{-1} and 1062 cm^{-1}. The vibration absorption was significantly weaker, showing that Fe^{3+} was successfully grafted to the sample by coordination with NH_2 (Godelitsas et al., 1999).

3.1.2 XRD analysis

The X-ray diffraction technique can accurately determine the crystal structure of substances and allows for the physical phase analysis of implications. Figure 3 shows the X-ray diffraction patterns of chitosan (CS) and iron-based modified chitosan powder (Fe-CS). It can be seen from the figure that the FeO(OH) standard card JCPDS 13-0518 is matched in the diffraction peak of Fe-CS. Among them can be identified distinct peaks 35.7°, 57.6°, and 62.9°, corresponding to the characteristic diffraction peaks of the (100), (102), and (110) crystal facets of FeO(OH) (Chen et al., 2021; Liu et al., 2023b), which indicates that Fe element was successfully in introduced into the sample.

3.1.3 SEM and EDS analysis

Scanning electron microscopy (SEM) was used to observe the microscopic morphology of the samples and the elemental composition of the surface area of the samples was analyzed through Energy dispersive spectrometry (EDS). The SEM results of chitosan (CS) and iron-based modified chitosan powder (Fe-CS) are shown in Figure 4. As can be seen from Figure 4A, the chitosan surface is relatively smooth and quite compact. After cross-linking with glutaraldehyde and chelating with $FeCl_3$, the morphology of iron-modified chitosan was significantly changed. The surface presents the appearance of folds, which may be caused by the Schiff base structure generated by the reaction between the aldehyde group and the amino group after the modification (Shkvarin et al., 2018). Comparing the microscopic morphology of the samples before and after modification, it can be found that the surface of the sample became rough and the folds increased, which was favorable in loading trivalent iron ions on the surface.

The elemental composition of the Fe-CS sample was analyzed by EDS and the results are shown in Figure 5. The mass fraction of the Fe element reached 24.5%, the highest mass fraction of the C element was 46.95%, and the mass fraction of the O element was 31.43%. Since the chitosan contains only C and O elements and no other impurity elements, a large amount of Fe was detected in the chitosan catalyst after loading with Fe^{3+}, indicating that Fe elements

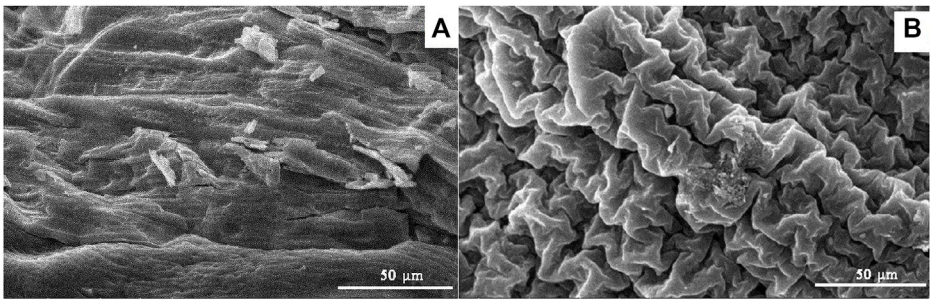

FIGURE 4
SEM photos of **(A)** CS and **(B)** Fe-CS.

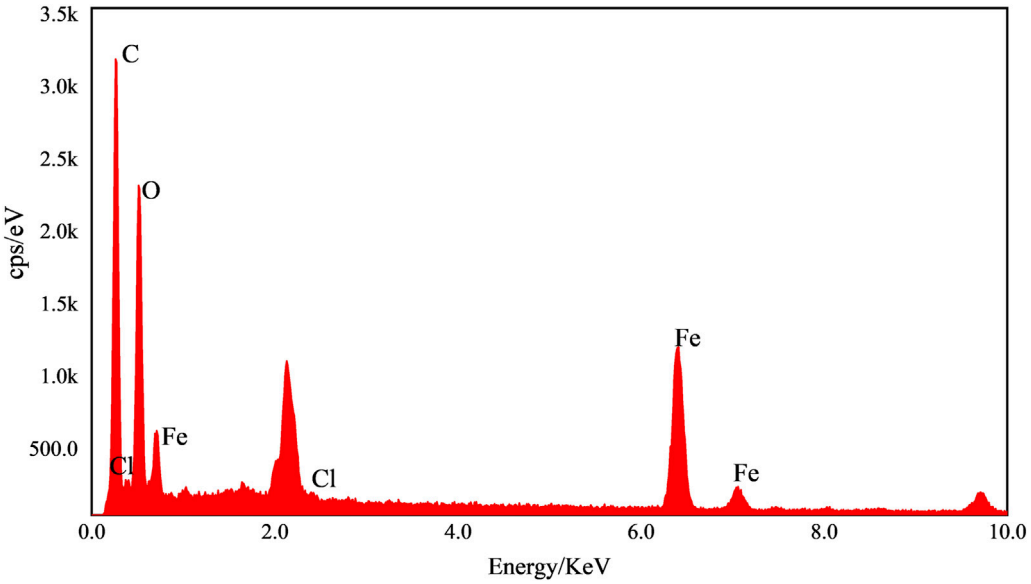

FIGURE 5
EDS analysis diagram of Fe-CS.

did chelate with chitosan and were successfully grafted on the chitosan surface.

3.2 Catalytic performance of Fe^{3+} modified chitosan

3.2.1 Effect of $FeCl_3$ dosage on the performance of modified chitosan catalysts

The amount of $FeCl_3$ dosing is an essential factor in the preparation of iron-based modified chitosan catalysts. Here, the catalytic regeneration reactions were carried out with m (CS)/m ($FeCl_3$) of 1/2, 1/5, and 1/8 to investigate the optimal ratios, respectively. 1 g of the prepared iron-based modified chitosan microspheres with different mass ratios was placed in a homemade U-shaped bubble tube, and oxygen was continuously introduced into the reactor at a gas rate of 300 ml/min. The mass ratio of 1/8 of the iron-based modified chitosan microspheres increased the density of the catalyst microspheres due to the excessive amount of $FeCl_3$, and the amount of oxygen introduced into the microspheres became smaller. The modified chitosan microspheres accumulated in the bottom of the U-shaped bubble tube and could not come in full contact with the desulfurization solution. The regeneration and desulfurization experiments were performed on the modified chitosan microspheres with mass ratios of 1/2 and 1/5 to determine the regeneration capacity of the catalyst. The desulfurization breakthrough curve after regeneration of the desulfurization solution in Figure 6 shows that the length of time to maintain the purification of the desulfurization solution after regeneration of the catalyst with the mass ratio of 1/2 is lower than that of the catalyst with the mass ratio of 1/5 under the same conditions, so the mass ratio of chitosan to $FeCl_3$ is chosen to be 1/5 for the subsequent experiments.

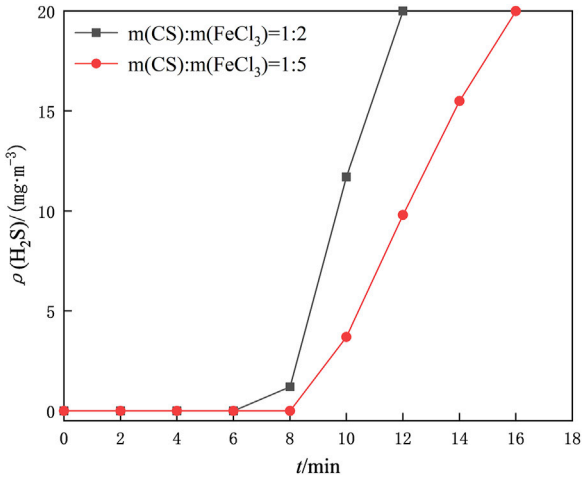

FIGURE 6
Comparison of desulfurization breakthrough time after regeneration of desulfurization fluid by modified chitosan microspheres prepared with different mass ratios of CS/$FeCl_3$.

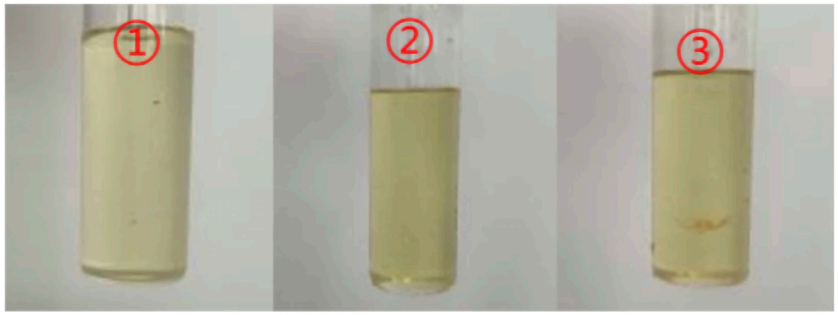

FIGURE 7
Comparison of the stability of modified samples with different mass fractions of glutaraldehyde in desulfurization solution (pictures from left to right are glutaraldehyde mass fractions of 12.5%, 5%, 2.5%).

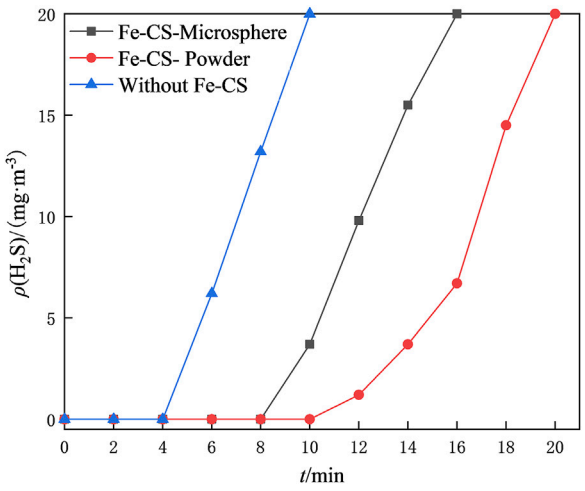

FIGURE 8
Effect of different forms of Fe-CS on the desulfurization capacity of the desulfurization solution after regeneration.

TABLE 1 Variation of ORP value of desulfurization solution after regeneration with different Fe-CS.

Sample	ORP/mV					ΔORP/mV
	0 h	1 h	2 h	3 h	4 h	
Fe-CS-Microsphere	88	106	130	131	134	46
Fe-CS- Powder	88	202	214	221	230	78
Without Fe-CS	88	91	92	96	96	8

3.2.2 Effect of glutaraldehyde dosage on the performance of modified chitosan catalysts

Glutaraldehyde, a commonly used cross-linking agent in the cross-linking process, was added to regulate the stability of modified chitosan microspheres. Here, 2.5%, 5%, and 12.5% of glutaraldehyde with mass percentages were used to prepare iron-based modified chitosan microspheres. 1 g of the prepared catalysts was added to the desulfurization solution and soaked for 24 h to observe whether the solution would change color due to the shedding of trivalent iron as the mass percent of glutaraldehyde added increased to determine whether the grafted Fe^{3+} was stable. As shown in Figure 7, the glutaraldehyde fraction of 12.5% was significantly stronger, and the solution was still clarified without discoloration. The catalyst with 5% loading was darker, and a small amount of solids were observed. The reason for this decolorization may be that the cross-linking with chitosan is weak when glutaraldehyde is not added in sufficient amounts, resulting in the weak adsorption of trivalent iron ions on the surface of modified chitosan (Xue and Liu, 2012). When the glutaraldehyde dosage was 12.5%, the trivalent iron attachment on the catalyst surface was more stable. However, a high dosage of glutaraldehyde would excessively consume the surface amino groups causing the reduction of active sites. In addition, a high glutaraldehyde dosage can lead to agglomeration of the synthesized catalysts and affect the dispersion and homogeneity of the catalysts (He et al., 2016), and thus a glutaraldehyde mass percentage of 12.5% is suitable.

3.2.3 Catalyst oxidation regeneration performance evaluation

To investigate the regeneration performance of the catalyst on the desulfurization waste solution, a static desulfurization experiment was conducted using 40 ml of homemade desulfurization solution, and the ORP values of the post-desulfurization system were measured. Two regeneration bulb tubes were taken, and 1 g of prepared iron-based modified chitosan microbeads and powdered catalysts were added. In addition, another bubble was added with desulfurization waste solution but without a catalyst as a blank control group. Oxygen was continuously injected into the three bubble tubes for 4 h at a flow rate was set of 300 ml/min for regeneration of the desulfurization waste solution, and the redox potential (ORP) of the upper clear solution was measured every 1 h. The regeneration performance of the catalyst on the desulfurization waste stream was investigated using the variation of the OPR value of the desulfurization solution and the desulfurization capacity of the regenerated desulfurization solution as the criteria. The mass concentration of H_2S in the exhaust gas was recorded at 2 min intervals, and the results are shown in Figure 8; Table 1. Table 1 shows that the difference in redox potential (ΔORP) of iron-based modified chitosan microspheres is 46 mV and that of modified chitosan powder is 78 mV after 4 h of regeneration, which indicates that the modified chitosan powder can oxidize the regenerated desulfurization waste stream more efficiently. In Figure 8, it can be seen that the H_2S concentration in the exhaust gas of desulfurization liquid regenerated by modified chitosan microspheres reached 20 mg/m^3 at 16 min, while that of modified chitosan powder reached 20 mg/m^3 at 20 min. This indicates that the desulfurization liquid regenerated by modified chitosan powder can absorb more H_2S in the same regeneration time, and the regeneration performance of modified chitosan powder is better compared with that of microspheres. This phenomenon may be due to the fact that the powdered catalyst has a more dispersed state and can be in full contact with the desulfurization solution (Lo et al., 2022). Due to the higher iron content and higher density of the microsphere catalyst, some of it accumulated at the bottom of the bubble tube during the regeneration process and could not fully contact the desulfurization solution. Accordingly, the regeneration effect was lower than that of the powdered catalyst. Compared with the blank control group, both showed higher ORP values, indicating that both have a certain catalytic ability and can effectively regenerate the desulfurization waste liquid.

3.2.4 Catalyst cycling performance

The reusability of catalysts is directly related to the service life and operating cost and is an essential indicator for evaluating the value of catalysts in practical applications (Graś et al., 2021). Here, the reusability and stability of the catalyst were evaluated by the sulfur capacity level of the desulfurization solution and the iron content on the catalyst after regeneration. After the catalyst is added to the desulfurization solution, the following oxidation-reduction reactions will occur in the solution (Liu et al., 2022; Qiu et al., 2022). Fe^{3+} oxidizes the H_2S originally absorbed by the coordination state to sulfur and removes it separately. After finishing, oxygen is passed to reoxidize Fe^{2+} on the catalyst to Fe^{3+}, thus the catalyst is regenerated.

1 Oxidation process

$$2Fe^{3+} + HS^{-}\ (\text{Coordination status}) \rightarrow 2Fe^{2+} + S\downarrow + H^{+} \quad (1)$$

2 Regeneration process (O_2)

$$2Fe^{2+} + 1/2O_2 + 2H^{+} \rightarrow 2Fe^{3+} + H_2O \quad (2)$$

The changes in the sulfur capacity of the desulfurization solution after regeneration are shown in Figure 9. The modified chitosan powder catalyst still maintained good catalytic performance after five times of reuse. The regenerated desulfurization solution always kept a purification time of about 18 min at higher H_2S concentrations. ICP examined the Fe content of the catalyst, and the difference in Fe content of the catalyst after five uses compared to the fresh catalyst did not exceed 1.5%, indicating that there was no excessive loss of active centers after five cycles. This can be attributed to the interaction between the carrier and Fe^{3+}, which enhances the stability of the catalyst. Overall, the iron-based catalysts prepared in this work have the advantages of stable composition and good reusability.

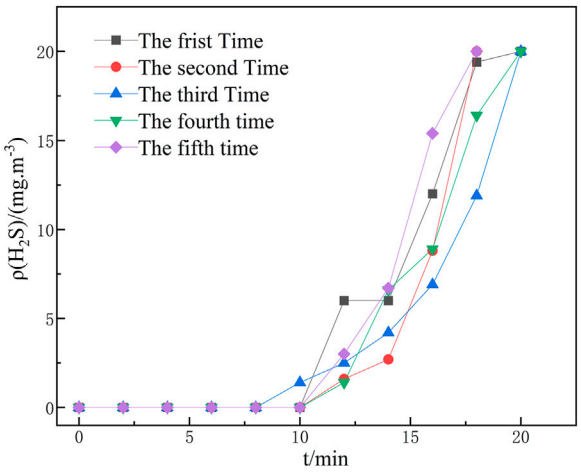

FIGURE 9
Desulfurization regeneration repeatability test results.

4 Conclusion

In this study, chitosan was used as the carrier, and glutaraldehyde was used as the cross-linking agent. The ferric ions were successfully grafted on the carrier through the coordination between the heteroatomic functional groups of chitosan and Fe^{3+} and used for the catalytic oxidative regeneration of desulfurized rich liquid. The catalyst morphology and structure were initially characterized using FTIR, XRD, SEM, EDS, and other characterization methods. The effects of varying the preparation conditions on the iron-based modified chitosan catalyst and the performance on the oxidative regeneration of the desulfurization solution were discussed. The effects of different morphologies of chitosan, $FeCl_3$ dosing, and glutaraldehyde dosing on the catalyst performance were investigated, respectively. The characterization results confirmed the successful loading of Fe^{3+} on chitosan. The desulfurization and regeneration experiments showed that the powdered iron-based modified chitosan catalyst had better catalytic performance than the microbead catalyst at a mass ratio of 1: 5 of chitosan to $FeCl_3$ and 12.5% mass fraction of glutaraldehyde. Overall, the strategy proposed in this work of selective catalytic oxidation of absorbed HS^- to monomeric sulfur by non-homogeneous oxidation enhancement effectively improves the sulfur blockage problem caused by the oxidation of sulfur monomers during the absorption process.

Data availability statement

The original contributions presented in the study are included in the article/supplementary material, further inquiries can be directed to the corresponding author.

Author contributions

ZL: Conceptualization, Methodology, Writing-Original draft, Validation, Resources, Review and editing. ZC: Review and editing. QC: Review and editing. LL: Data curation, Investigation. YW: Editing. PS: Data curation. YZ: Data curation. ZS: Data curation. KQ: Supervision.

Funding

The research was funded by China National Science and Technology Major Project (2016ZX05017) and the Sinopec Group Corporation 2020 Science and Technology Project "Organic Sulfur Catalytic Hydrolysis Technology Improves Quality Research" (No.120049-1).

Conflict of interest

The authors declare that the research was conducted in the absence of any commercial or financial relationships that could be construed as a potential conflict of interest.

Publisher's note

References

Chen, Z., Zheng, R., Graś, M., Wei, W., Lota, G., Chen, H., et al. (2021). Tuning electronic property and surface reconstruction of amorphous iron borides via W-P co-doping for highly efficient oxygen evolution. *Appl. Catal. B Environ.* 288, 120037. doi:10.1016/j.apcatb.2021.120037

Godelitsas, A., Charistos, D., Dwyer, J., Tsipis, C., Filippidis, A., Hatzidimitriou, A., et al. (1999). Copper(II)-loaded HEU-type zeolite crystals: Characterization and evidence of surface complexation with N,N-diethyldithiocarbamate anions. *Microporous Mesoporous Mater.* 33, 77–87. doi:10.1016/S1387-1811(99)00124-9

Graś, M., Kolanowski, Ł., Chen, Z., Lota, K., Jurak, K., Ryl, J., et al. (2021). Partial inhibition of borohydride hydrolysis using porous activated carbon as an effective method to improve the electrocatalytic activity of the DBFC anode. *Sustain. Energy Fuels* 5, 4401–4413. doi:10.1039/D1SE00999K

Gu, Z., Xiang, X., Fan, G., and Li, F. (2008). Facile synthesis and characterization of cobalt ferrite nanocrystals via a simple Reduction–Oxidation route. *J. Phys. Chem. C* 112, 18459–18466. doi:10.1021/jp806682q

He, X., Li, K., Xing, R., Liu, S., Hu, L., and Li, P. (2016). The production of fully deacetylated chitosan by compression method. *Egypt. J. Aquatic Res.* 42, 75–81. doi:10.1016/j.ejar.2015.09.003

Liu, Z., Qiu, K., Dong, Y., Jin, Z., Liu, L., and Wu, J. (2022). Sb-Fe bimetallic non-aqueous phase desulfurizer for efficient absorption of hydrogen sulfide: A combined experimental and dft study. *Korean J. Chem. Eng.* 39, 3305–3314. doi:10.1007/s11814-022-1253-6

Liu, Z., Qiu, K., Sun, G., Ma, Y., Wang, Y., Peng, J., et al. (2023). Aminated polyacrylonitrile fibers for the removal of hydrogen sulfide from natural gas at room temperature. *Res. Chem. Intermed.* 49, 701–716. doi:10.1007/s11164-022-04897-1

Liu, Z., Sun, G., Chen, Z., Ma, Y., Qiu, K., Li, M., et al. (2023). Anchoring Cu-N active sites on functionalized polyacrylonitrile fibers for highly selective H_2S/CO_2 separation. *J. Hazard. Mater.* 450, 131084. doi:10.1016/j.jhazmat.2023.131084

Lo, R., Manna, D., Lamanec, M., Dračínský, M., Bouř, P., Wu, T., et al. (2022). The stability of covalent dative bond significantly increases with increasing solvent polarity. *Nat. Commun.* 13, 2107. doi:10.1038/s41467-022-29806-3

Mohammadi, A., Saadati, Z., and Joohari, S. (2019). Comparison of the adsorption of H_2S by ZnO–TiO_2 and Ni–ZnO–TiO_2 nanoparticles: An adsorption isotherm and thermodynamic study. *Environ. Prog. Sustain. Energy* 38. e13258. doi:10.1002/ep.13258

Qiu, K., Liu, Z., Dong, Y., Liu, L., Li, W., Niu, S., et al. (2022). [Bmim]$FeCl_4$ efficient catalytic oxidative removal of H_2S by Cu^{2+} synergistic reinforcement. *Chem Eng Technol* 45, 1867–1875. doi:10.1002/ceat.202200235

Ren, Z., Shen, Y., Gao, H., Chen, H., Liu, C., and Chen, Z. (2021). Comparison of sodium oleate and sodium petroleum sulfonate for low-temperature flotation of fluorite and the collecting mechanisms. *Min. Metallurgy Explor.* 38, 2527–2536. doi:10.1007/s42461-021-00494-9

Shkvarin, A. S., Merentsov, A. I., Titov, A. A., Yarmoshenko, Yu.M., Shkvarina, E. G., Píš, I., et al. (2018). Quasimolecular complexes in the $Cu_xTiSe_{2-y}S_y$ intercalation compound. *J. Mat. Chem. C* 6, 12592–12600. doi:10.1039/C8TC04115F

Vogt, C., and Weckhuysen, B. M. (2022). The concept of active site in heterogeneous catalysis. *Nat. Rev. Chem.* 6, 89–111. doi:10.1038/s41570-021-00340-y

Wang, Y., Yang, C., Zhang, C., Duan, M., Wang, H., Fan, H., et al. (2022). Effect of hierarchical porous MOF-199 regulated by PVP on their ambient desulfurization performance. *Fuel* 319, 123845. doi:10.1016/j.fuel.2022.123845

Xue, Q., and Liu, Y. (2012). Removal of minor concentration of H_2S on MDEA-modified SBA-15 for gas purification. *J. Industrial Eng. Chem.* 18, 169–173. doi:10.1016/j.jiec.2011.11.005

Zheng, R., Gao, H., Ren, Z., Cen, D., and Chen, Z. (2017). Preparation of activated bentonite and its adsorption behavior on oil-soluble green pigment. *Physicochem. Problems Mineral Process.* 53 (2), 829–845. doi:10.5277/ppmp170213